



Synergistic anticancer activity of dietary tea polyphenols and bleomycin hydrochloride in human cervical cancer cell: Caspase-dependent and independent apoptotic pathways



Ali A. Alshatwi^{*}, Vaiyapuri Subbarayan Periasamy, Jegan Athinarayanan, Ramesh Elango

Nanobiotechnology and Molecular Biology Research Lab, Department of Food Science and Nutrition, College of Food and Agriculture Sciences, King Saud University, Riyadh, Saudi Arabia

ARTICLE INFO

Article history:

Received 12 October 2015

Received in revised form

14 December 2015

Accepted 15 January 2016

Available online xxx

Keywords:

Synergistic effect

Cervical cancer

Apoptosis

Bleomycin

Tea polyphenols

ABSTRACT

Bleomycin is a chemotherapeutic agent that is frequently used in the treatment of various cancers. Bleomycin causes serious adverse effects via antioxidant defense abnormalities against reactive oxygen species (ROS). However, the current cervical cancer monodrug therapy strategy has failed to produce the expected outcomes; hence, combinational therapies are gaining great interest. Tea polyphenols are also effective antioxidative and chemo-preventive agents. However, the combined effect of tea polyphenol (TPP) and bleomycin (BLM) against cervical cancer remains unknown. In this study, we focused on the potential of TPP on BLM anticancer activity against cervical cancer cells. Cervical cancer cells (SiHa) were treated with various concentrations of TPP, BLM and TPP combined with BLM (TPP-BLM), and their effects on cell growth, intracellular reactive oxygen species, poly-caspase activity, early apoptosis and the expression of caspase-3, caspase-8 and caspase-9, Bcl-2 and p53 were assessed. The MTT assay revealed that the SiHa cells were less sensitive to growth inhibition by TPP treatment compared with both BLM and the combination therapy. Nuclear staining indicated that exposure to TPP-BLM increased the percentage of apoptotic nuclei compared with a mono-agent treatment. Caspase activation assay demonstrated that proportion of early and late apoptotic/secondary necrotic cells was higher in the cells treated with the combination therapy than in those treated with either TPP or BLM alone. The TPP-BLM treatment synergistically induced apoptosis through caspase-3, caspase-8 and caspase-9 activation, Bcl-2 upregulation and p53 overexpression. This study suggests that TPP-BLM may be used as an efficient antioxidant-based combination therapy for cervical cancer.

© 2016 Elsevier Ireland Ltd. All rights reserved.

1. Introduction

Cervical cancer is the fourth most frequent malignancy that affects women worldwide; it has been estimated that 528,000 new cases occurred in 2012. According to a cancer incidence and survival report of Saudi Arabia 2007, cervical cancer is the 13th most prevalent cancer in Saudi women. The World Health Organization (WHO) predicts that future cervical cancer rates could considerably increase in Arab countries, including Saudi Arabia [1–3]. The molecular mechanism of cervical cancers is a multifaceted problem, and it is mostly associated with human papilloma virus (HPV)

infection; HPV integration into the host cell's genome leads to its involvement in several regulatory gene networks. Therefore, both internal and external factors are involved in the initiation and progression of cervical cancer. The cell cycle and the apoptotic pathway dysregulation contribute to the initiation and progression of cervical cancer. A few crucial HPV oncoproteins cause immortalization of the infected cells by interacting with and degrading p53, cell cycle regulator proteins and the mitochondrial mediated redox pathway proteins [4,5]. In general, the majority of the HPV oncoproteins, apoptotic signal transduction and redox related genes are disrupted by mutations and epigenetic changes in these regulatory networks [5–8].

Currently, various methods are available for HPV positive cervical cancer treatment, including surgery, chemotherapy and radiotherapy, although these methods have apparent drawbacks. The NCI-approved cancer drugs include bevacizumab, bleomycin,

^{*} Corresponding author. Department of Food Science and Nutrition, College of Food and Agriculture Sciences, King Saud University, P.O. Box 2460, Riyadh 11451, Saudi Arabia.

E-mail address: nano.alshatwi@gmail.com (A.A. Alshatwi).

cisplatin and topotecan; however, these drugs lack specific targets, which leads to normal cell damage, myelotoxicity, nervous tissue injury, diarrhea and renal failure [9,10]. Most of these drugs generate high-level free radicals or metabolic intermediates that induce oxidative damage to DNA in normal cells and lead to chemoresistance through anti-apoptosis mechanisms. For instance, bleomycin (BLM), an anti-neoplastic antibiotic based chemotherapeutic agent that is produced by *Streptomyces verticillus*, and it is used primarily to treat various types of redox-influenced cancer, including testicular cancer, lymphoma, and squamous cell cancer of the head, neck and cervix [11]; however, it can cause several health illnesses. Fig. 1A shows chemical structure of bleomycin. BLM is a glycopeptide that complexes with iron and generates high-level superoxides and hydroxyl radicals that induce oxidative damage

to DNA and leads to cancer cell proliferation inhibition [12]. BLM has a metal binding region that easily coordinates with metal ions to form metallo bleomycin complexes [13], which are mechanistically involved in cellular level DNA damage. For instance, in the presence of cellular level redox active metal ions or oxygen BLM, cancer cell DNA degradation was induced [14,15]. The molecular mechanism of BLM-induced mitochondrial dysregulation in various cancers is believed to be oxidative stress-mediated DNA damage [16–19]. However, BLM monotherapy can cause different adverse events, including immune system damage, hyperpigmentation, pneumonitis and pulmonary fibrosis, which are mediated by redox status disturbances [20,21].

Combinational chemotherapy is the use of more than one medication, and this procedure can overcome the disadvantages

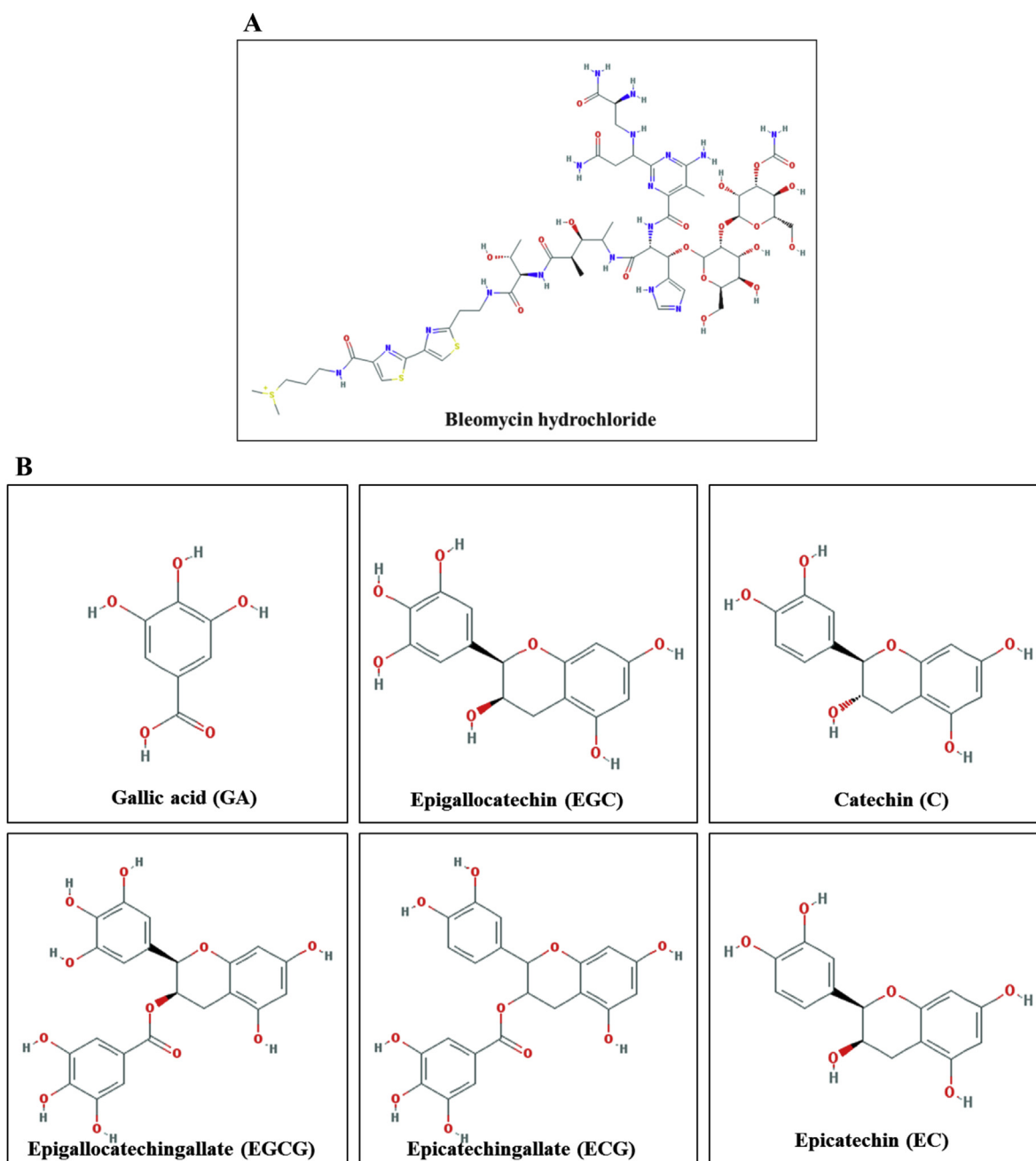


Fig. 1. Chemical structure of (A) Bleomycin hydrochloride and (B) Tea polyphenols.

of the monotherapy and show significant promise in cancer therapy. Recently, drug and phytochemical combined cancer therapies have received a great deal of attention because drug and phytochemical interactions can either enhance (synergize) or decrease (antagonize) therapeutic effects. Additionally, dietary supplements can reduce cancer risk, prolong cancer patient survival times and decrease chemotherapy-associated side effects [22,23]. A few recent studies demonstrated that dietary phytochemicals could eliminate the toxic side effects of synthetic drugs. Kaiserova et al. demonstrated that flavonoids are excellent agents for relieving doxorubicin-induced cardiac side-effects [24]. Scambia et al. reported that quercetin significantly enhanced the growth-inhibitory effect of adriamycin in multi-drug resistant cancer cells [25]. Hoffman et al. suggested a flavonoid enhanced anti-proliferative action of busulphan on a human leukemia cell line [26]. Additionally, when BLM was used with phytochemicals in combinational therapies, the phytochemicals significantly increased the BLM efficiency and reduced its side effects [16,27]. Hence, efforts have been expended to develop a synergistic combination therapy using drugs and phytochemicals that prevent redox-mediated toxicity and enhance treatment efficiency.

Tea polyphenols (TPP) are potential antioxidants that scavenge reactive oxygen and nitrogen species and chelate redox-active transition metal ions [27]. TPP contains several catechin compounds, including (-)- epigallocatechin-3-gallate (EGCG), (-)- epigallocatechin (EGC), epicatechin-3-gallate (ECG), and other catechins (Fig. 1B) that have a wide range of biological properties, such as anti-cancer, anti-allergic, anti-inflammatory, and cancer chemoprevention activities [28–30]. TPP is a very promising substance for various cancer treatment types because it inhibits carcinogenesis and cancer cell proliferation at various organ sites [29]. Several reports have demonstrated that TPP contains antioxidants that can neutralize excessive free radicals (ROS) and may reduce or even help prevent some of the intracellular damage that they cause [30–32]. Sriram et al. suggested tea epigallocatechin-3-gallate as a potential anti-fibrotic agent because of its ability to attenuate BLM-induced pulmonary fibrosis [33].

The complete health benefits of green tea polyphenols that have been observed so far have not focused on the combined activities of TPP with BLM in comparison with single compound treatments. Hence, it is possible that by targeting direct- or indirect-acting pro- and antioxidants and redox modulators, such as TPP, with BLM, they will act as central redox system co-ordinators of anti-apoptotic and ROS signaling networks. At the same time, the best way to increase the efficacy, pharmacokinetics and selectivity and to reduce BLM toxicity of BLM is to combine it in treatment with TPP. However, the current molecular-based evidence is inadequate regarding the clinical and patient guideline determinations of TPP use as an antioxidant supplement during cervical cancer therapy. In this context, *in vitro*-based approaches were applied to understand whether specific modes of cell death (e.g., apoptosis, autophagy, necro-apoptosis) were the mechanisms by which synergistic combination screens killed targeted tumor cells, and if so, the likely molecular mechanism(s) by which they participate.

2. Materials and methods

2.1. Cell culture

Cervical cancer cell (SiHa) was procured from the National Centre for Cell Science (NCCS), Pune, India and provided by Prof. M.A. Akbarsha of the Mahatma Gandhi-Doerenkamp Center for

Alternatives to Use of Animals in Life Science Education, Bharathidasan University, India. The cells were grown in DMEM medium that was supplemented with 10% fetal bovine serum (HyClone, Thermo Scientific, USA), and 100 U/mL penicillin and 100 µg/mL streptomycin were used as antibiotics (HyClone, Thermo Scientific, USA). The cells were grown in T25 and T75 cm² flasks as well as 6-, 12-, 24- or 96-well culture plates (TPP, Switzerland) at 37 °C in a humidified atmosphere containing 5% CO₂ in a CO₂ incubator (Biochrom AG, Germany). All of the experiments were achieved using cells from passage 15 or below. The culture conditions of the SiHa cells were consistent for all of the experiments described below.

2.2. Cell viability assay

The TPP and BLM stock solutions were prepared with DMSO. Further working solutions were prepared in the DMEM growth media. The SiHa cells were seeded at a density of 1×10^4 cells per well in 200 µL of fresh culture media. After overnight growth, the SiHa cells were treated with different TPP and BLM working solution concentrations for 24 h. After incubation, 20 µL of MTT solution (5 mg/mL in phosphate buffered saline, Sigma–Aldrich, USA) was added to each well, and the plates were wrapped with aluminum foil and incubated at 37 °C for 6 h. The plates were centrifuged at 4000 rpm for 5 min, and the purple formazan product was dissolved in 100 µL of 100% DMSO. The absorbances were monitored at 570 nm (measurement) and 630 nm (reference) with a multiwell plate reader (Bio-Rad, USA). The data were collected in quadruplicate for each dose (as technical replicates), and two independent experiments ($n = 2$) in order to calculate the median-effect dose (i.e., the IC_{50Dm} value), to measure dose-effect curve sigmoidicity (m value), to determine the median-effect plot linear correlation coefficient (r value), and for the drug-combinational analysis using the CalcuSyn software (Biosoft, UK).

2.3. Experimental design for the drug combinations

A cytotoxic assay was performed for TPP and BLM to obtain dose effect parameters, such as the median dose (Dm)₁, sigmoidity (m)₁, and correlation coefficient (r)₁ of TPP alone and the median dose (Dm)₂, sigmoidity (m)₂, and correlation coefficient (r)₂ of BLM alone for the dose-effect curves and median effect plot, using the CalcuSyn software. The SiHa cells were exposed to different TPP (Control, 25, 50, 75, 100, and 125 µg/mL) and BLM (Control, 5, 10, 15, 20, and 25 µM/mL) concentrations for 24 h. The cell death percentages, (IC₂₅, IC₅₀, and IC₇₅), and dose effective parameters were calculated with the CalcuSyn software. For the combination studies, in which the MTT assay was conducted for the TPP-BLM treatment analysis, three combination mixture data points were used to determine the combination index (CI) value and the isobologram analysis. For the combination analysis, the SiHa cells were treated with TPP at different concentrations (Control, 25, 50, 75, 100, and 125 µg/mL) and in combination with BLM at fixed concentrations at three different points (TPP IC₅₀ + BLM IC₂₅ and TPP IC₇₅ + BLM) for 24 h, and the cell viability was determined using the MTT assay. Then, the data were subjected to a combination analysis. The CI was calculated with the Chou and Talalay combination index equation [34]. $CI < 1$, $CI = 1$, and $CI > 1$ indicated synergism, additive effect, and antagonism, respectively. A normalized isobologram analysis was conducted to illustrate the additivity, synergism, or antagonism of the various combination doses. If the combination data point for $fa = 0.5$ fell on the diagonal line, then an additive effect was indicated; if it fell in the lower left region, then synergism was indicated; and if it fell in the upper right region, then antagonism was indicated. The synergistic combination dose was selected

based on the lowest CI value and isobologram analysis, and it was applied for all of the experiments described below.

2.4. Propidium iodide staining

The effects of TPP, BLM and TPP-BLM on the morphological features of the SiHa cells were analyzed using propidium iodide (PI) staining. The cells were treated with TPP (IC₅₀ dose), BLM (IC₅₀ dose) and a synergistic combination dose (TPP IC₅₀ + BLM IC₂₅ and TPP IC₇₅ + BLM IC₂₅) in DMEM medium for 24 h at 37 °C. The cell nuclear morphologies were observed by staining the DNA content of trypsinized cells (4.0×10^4 /mL) with 10 μ L of PI stain (100 μ g/mL, aqueous, Promega, USA and Sigma, USA) for 5 min at 37 °C. A drop of cell suspension was placed on a glass slide and a coverslip was placed over the slide to reduce light diffraction. The cells were photographed at random with a fluorescent microscope at 400x magnification (Carl Zeiss, Jena, Germany). Data were derived from at least three independent experiments (n = 3) with technical replicates (n = 3 slides).

2.5. ROS measurements

The intracellular reactive oxygen species (ROS) level was analyzed using the fluorescent probe, 6-carboxy-2',7'-dichlorodihydrofluorescein diacetate, di(acetoxymethyl ester) as per the manufacturer's instructions (Invitrogen, USA). This reagent readily diffuses through the cell membrane and is enzymatically hydrolyzed by intracellular esterases to form the non-fluorescent compound, 2',7'-dichlorofluorescein (DCFH), which is then rapidly oxidized to form the highly fluorescent compound, 2',7'-dichlorofluorescein (DCF) in the presence of ROS. The fluorescence intensity

of DCF is an indicator of the amount of intracellular ROS. To determine the total intracellular ROS levels of the untreated SiHa cells (control) and those treated with TPP, BLM and TPP-BLM, the cells were seeded in 12-well plates on the day prior to the assay. The cells were treated with a TPP (IC₅₀), BLM (IC₅₀ dose) or a synergistic TPP-BLM dose (TPP IC₅₀ + BLM IC₂₅ and TPP IC₇₅ + BLM IC₂₅) in DMEM medium for 24 h at 37 °C. After the 24-hr incubation, the medium was removed, and the cells were washed with PBS and then incubated with a 10 μ M probe in the loading medium. After the probe was removed, the cells were washed and incubated with PBS. The intracellular fluorescence intensity with 10,000 events was measured using a BD FACSCalibur (BD Biosciences, USA) on the FL-1 channel. The acquired data were analyzed with the BDCellQuest Pro software. The data were collected in triplicates for each dose (as technical replicates).

2.6. Polycaspase apoptosis assay

To analyze the polycaspase activity of the untreated (control) and the TPP, BLM or TPP-BLM treated SiHa cells, the cells were plated on 12-well plates on the day prior to the assay. The cells were exposed to TPP (IC₅₀), BLM (IC₅₀) or synergistic TPP-BLM doses (TPP IC₅₀ + BLM IC₂₅ and TPP IC₇₅ + BLM IC₂₅) in DMEM medium for 24 h. After 24 h, the cells were harvested, resuspended, and stained with the FLICA reagent for polycaspases and propidium iodide with the Vybrant FAM PolyCaspases Assay Kit (Invitrogen, USA). Ten thousand events were acquired on a FACScanto II flow cytometer at a 488-nm excitation wavelength, with 530-nm band pass and 670-nm long pass emission filters. The acquired data were analyzed using the BD FACSDiva and BDCellQuest Pro software. The data were collected in triplicates for each dose (as technical replicates).

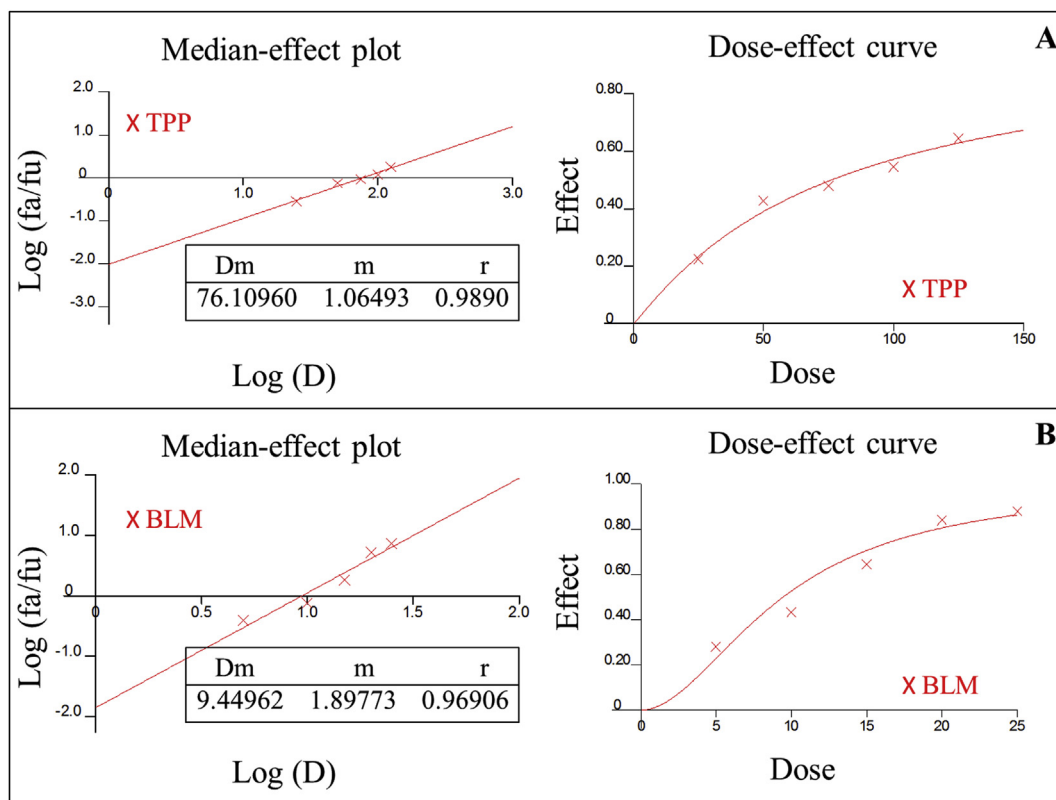


Fig. 2. The *in vitro* cytotoxicity effects of TPP and BLM alone in cervical cancer cells. Cervical cells were treated with different concentrations of (A) TPP and (B) BLM alone. After 24 h of exposure, the cell death percentage was determined with an MTT assay to determine the IC₂₅, IC₅₀, IC₇₅, m value (a measurement of the sigmoidity of the dose–effect curve), and r value (the linear correlation coefficient of the median–effect plot), which were calculated with the Calcsyn software.

2.7. Gene expression analysis

To determine the mRNA levels of the untreated (control) and TPP, BLM and TPP-BLM treated SiHa cells, the cells were seeded on 24-well plates on the day prior to the assay. The cells were incubated with TPP (IC₅₀), BLM (IC₅₀) and synergistic TPP-BLM doses (TPP IC₅₀ + BLM IC₂₅ and TPP IC₇₅ + BLM IC₂₅) in DMEM medium for 24 h at 37 °C. Total RNA from cells was extracted, and cDNA was synthesized with the FastLane Cell cDNA Kit (Qiagen, USA). The cycle parameters for the RT reactions were 42 °C for 5 min, 42 °C for 30 min, 85 °C for 5 min, and then the samples were held at 4 °C. Quantitative PCR was performed with a RT-PCR kit (Qiagen, USA) and analyzed on a Real-Time PCR workstation (AB Biosciences, USA). Quantitect Primer assays for the genes of interest (caspases-3, -8 and -9, p53 and GAPDH) were chosen and purchased from Qiagen (USA). The PCR reaction mix consisted of the RT product, primer and probe for the gene of interest and was cycled in accordance with the manufacturer's instructions for the QuantiFast SYBR Green PCR kit (Qiagen). The cycle parameters for the PCR reaction were 95 °C for 5 min, followed by 40 cycles of a 95 °C denaturing step for 10 seconds and an annealing/extension step at 60 °C for 30 seconds. The relative mRNA levels in each sample were normalized to the GAPDH content. Quantitative values were obtained from the threshold PCR cycle number (Ct), at which the increase in signal associated with an exponential increase of the PCR product was detected. In each sample, we calculated the ΔC_T values (target-reference). The fold-change between the control (untreated) and TPP, BLM or TPP-BLM treated samples for p53 and

caspase-3, -8, and -9 were calculated with the $2^{-\Delta\Delta C_T}$ method, in which $\Delta\Delta C_T = \Delta C_T$ (target-reference) (in the TPP, BLM or combination treated samples) - ΔC_T (target-reference) (in untreated samples). Real-time PCR was repeated in triplicate for each sample, and the average $2^{-\Delta\Delta C_T}$ values and their S.D. were calculated for each sample relative to the normal control for the p53 and caspase-3, -8, and -9 expression levels. GAPDH was used as reference gene. The p53 and caspase-3, -8, and -9 expression levels were normalized to a reference gene (GAPDH). The data were collected in triplicates for each dose (as technical replicates) and two independent experiments (n = 2).

2.8. Protein interaction network analysis

BLM and TPP altered proteins and/or genes details were obtained from previous experiments, databases and literatures. The protein interaction network was constructed using Stitch 4.0 and Cytoscape 3.2. Bleomycin (BLM), catechins and gallic acid associated protein interaction network map, and gene ontology (GO) enrichment and pathway analysis were assessed using STITCH 4.0 database.

2.9. Statistical analysis

The results are expressed as the mean \pm standard deviation (SD). All of the data were derived from at least three independent experiments with a similar pattern. The statistical analyses of the experimental data were performed using the Microsoft Excel and CalcuSyn software. For all of the comparisons, the differences were

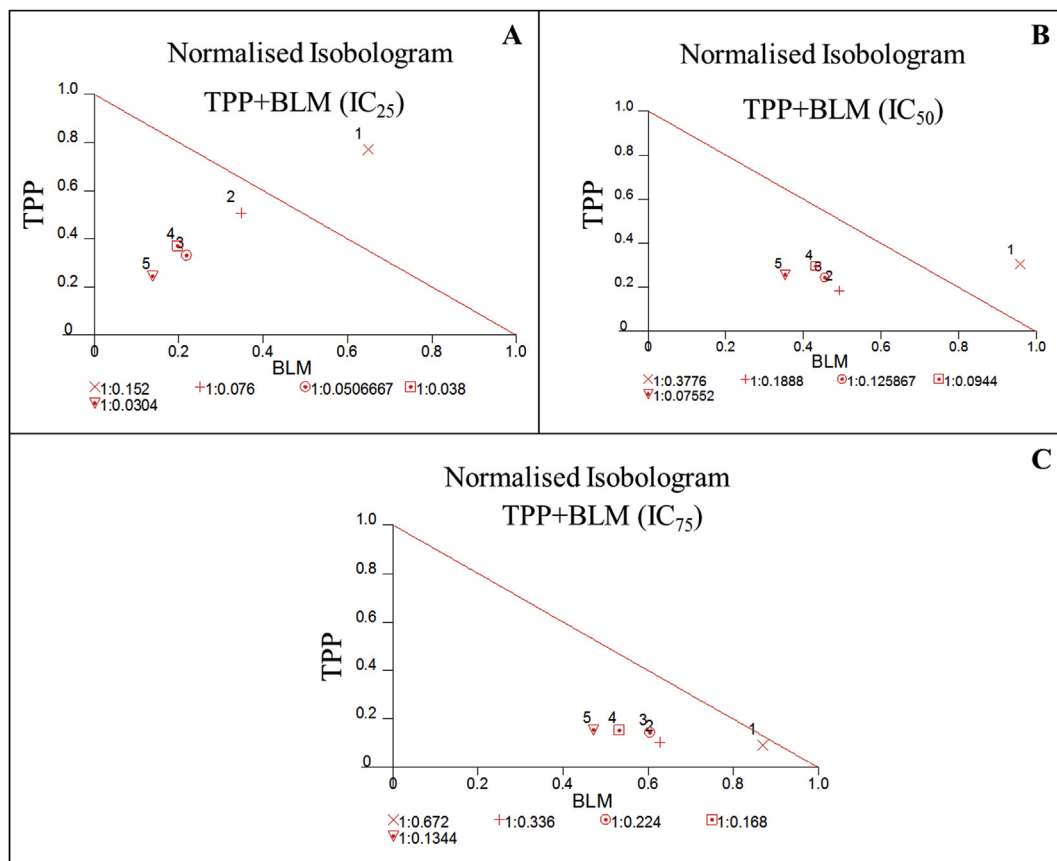


Fig. 3. Normalized isobologram graphs of TPP at various concentrations (Control, 25, 50, 75, 100, 125 µg/mL) and in combination with (A) IC₂₅ (B) IC₅₀ (C) IC₇₅ value of BLM were produced to illustrate additivity, synergism, or antagonism. If the combination data point for fa = 0.5 fell on the diagonal line, then an additive effect was indicated; if it fell in the lower left, then synergism was indicated; and if it fell in the upper right region, then antagonism was indicated. The data from the three different combinations fell in the lower left region of the normalized isobolograms.

considered statistically significant at $p < 0.05$.

3. Results

3.1. Cytotoxicity with BLM and TPP combination treatments

To assess the dose-dependent cytotoxic properties of TPP and BLM in SiHa cells, the cells were exposed to semi-log doses of TPP or BLM alone. After the 24-hr incubations, the cell viability was assessed, and the inhibitory concentrations were calculated as follows: TPP, $IC_{25} = 27 \mu\text{g/mL}$, and $IC_{50} = 76 \mu\text{g/mL}$ and $IC_{75} = 98.1 \mu\text{g/mL}$; BLM, $IC_{25} = 3.8 \mu\text{M}$, $IC_{50} = 9.44 \mu\text{M}$ and $IC_{75} = 16.8 \mu\text{M}$. Then, the cells were exposed to the TPP-BLM combinations, and the BLM concentrations were fixed at three different points for 24 h. The combinations index (CI) and isobologram analyses were performed using the CalcuSyn software to analyze the synergistic effects of the various TPP and BLM combinations. The results showed that the TPP and BLM doses inhibited the SiHa cell viability in a dose-dependent manner (Fig. 2 A and B). The median TPP dose effect plots with the three different BLM concentrations demonstrated that combination treatments were more effective than were TPP and BLM alone in the SiHa cells (Supporting data: Figs. S1, S2 and S3). The CI values of the three different combinations were less than 1.0, which clearly revealed a synergistic effect. The (TPP + BLM- IC_{25}), (TPP + BLM- IC_{50}) and (TPP + BLM- IC_{75}) CI values showed clear synergism in the ranges of 0.382–1.421, 0.611 to 1.264 and 0.62 to 0.96, respectively, in the SiHa cells. Moreover, a normalized isobolographic analysis clearly

showed a synergistic pattern, as the data point for $f_a = 0.5$ fell in the lower left region of the graph (Fig. 3). The synergistic combination dose was selected based on CI value and isobologram analysis (TPP IC_{50} + BLM IC_{25} and TPP IC_{75} + BLM IC_{25}), and this dose was applied for all of the experiments described below.

3.2. PI staining

The TPP, BLM and TPP-BLM combinations treated SiHa cells were observed under fluorescence microscopy following PI staining. The microscopic observations revealed that TPP, BLM and TPP-BLM treatments caused chromatin fragmentation, nuclear shrinkage, cytoplasmic vacuolation, cytoplasmic blebbing, binucleation and late apoptosis in the SiHa cells (Fig. 4). These nuclear morphological changes confirmed that the cells were committed to cell death through apoptosis rather than necrosis. The microscopic analysis showed that the percent of cells with apoptotic morphologies increased significantly when the cells were treated with TPP-BLM compared with either TPP or BLM alone.

3.3. Intracellular ROS level changes

The SiHa cells were exposed to TPP, BLM and TPP-BLM combinations for 24 h. After incubation, the intracellular ROS level was analyzed. The ROS level histogram patterns revealed that the BLM treatment enhanced the high-level ROS generation, whereas TPP suppressed the ROS generation levels dose-dependently. Fig. 5 clearly revealed that a major peak shift in the histogram overlap

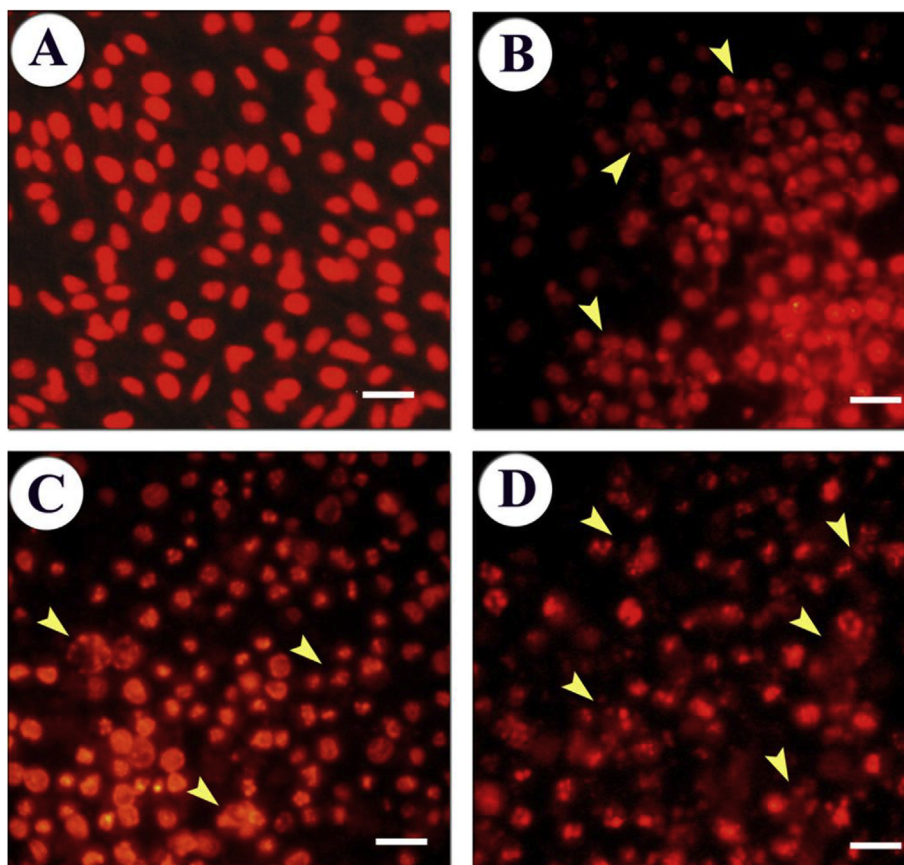


Fig. 4. Fluorescent microscopy images of the TPP, BLM and or TPP + BLM treated cells and the untreated control cells. Cervical cells were incubated with TPP IC_{50} , BLM IC_{50} or a synergistic combination dose (TPP IC_{50} + BLM IC_{25} and TPP IC_{75} + BLM IC_{25}) for 24 h. Propidium iodide-stained SiHa cancer cells that were untreated (A) or treated with TPP (B), BLM (C) or a TPP + BLM combination (D) for 24 h (400x magnification). The yellow arrowheads point to cells with abnormal nuclei and indicate nuclei/chromatin fragmentation. (For interpretation of the references to colour in this figure legend, the reader is referred to the web version of this article).

between the BLM-induced high ROS generation and the TPP anti-oxidants effects. This is understandable because TPP is a potential antioxidant.

3.4. Caspase activation

Caspases are present as intracellular inactive pro-enzymes, which are responsible for the deliberate disassembly of the cell into apoptotic bodies during apoptosis. These enzymes participate in a sequence of reactions that are stimulated from proapoptotic signals and result in the cleavage of protein substrates and the subsequent disassembly of the cellular system. Here, we observed the TPP, BLM and TPP-BLM combinations treatment effects on the SiHa cells for 24-hr. Based on the fluorochrome binding differences, four different populations were distinguished on the bivariate PI versus FAM scatter plots. As shown in Fig. 6, the cells were classified into four different types: normal (FLICA-/PI-), early apoptotic (FLICA+/PI-), late apoptotic (FLICA+/PI+), secondary necrotic, and necrotic cells (FLICA-/PI+). The early and late apoptotic populations were significantly increased in the TPP-BLM treated SiHa cells (TPP IC₂₅ in µg/mL + BLM IC₂₅ in µM/ml) compared with the single TPP or BLM treatments.

3.5. Gene expression analysis by qPCR

The SiHa cells were treated with TPP, BLM and TPP-BLM combinations for 24 h. The caspase-3, -8 and -9 and p53 mRNA levels were quantified. As shown in Fig. 7, the average $2^{-\Delta\Delta Ct}$ values along their SDs were calculated for each sample relative to the untreated control for the p53 and caspase-3, -8, and -9

expression levels. The results are presented as the mean \pm SD, and $*p < 0.05$ was considered significant when the individual TPP and BLM treatments were compared with the synergistic combination dose (TPP IC₅₀ + BLM IC₂₅ and TPP IC₇₅ + BLM IC₂₅) after a 24-hr incubation. The values represent the p53 and caspase-3, -8 and -9 mRNA levels in the SiHa cells that were treated with the TPP, BLM or synergistic combination doses (TPP IC₅₀ + BLM IC₂₅ and TPP IC₇₅ + BLM IC₂₅) (Fig. 7). With the combination treatment, the p53 transcript levels in the SiHa cells significantly increased by approximately two fold following 24 h of incubation compared with the individual TPP or BLM treatments ($p < 0.05$). According to Livak's calculation, the effector caspase-3 and initiator caspase-8 mRNA expression levels were upregulated with the synergistic combination dose (TPP IC₅₀ + BLM IC₂₅ and TPP IC₇₅ + BLM IC₂₅) by four- and three-fold, respectively, whereas the caspase-9 levels increased two-fold (Fig. 7). Moreover, the BCL-2 expression levels significantly increased (four-fold) in the TPP and BLM combined treated cells compared with the TPP or BLM single treatments. These results suggest that combined drug therapy can inhibit cancer cell proliferation to a higher degree compared with mono-drug therapy.

4. Discussion

Synergistic target-based combinations can affect or repair independent cancer growth stimulatory signals, PCD resistance, and overcome hypoxia-mediated cellular senescence in the crucial regulatory and metabolic pathways of cancer cells [11,35,36]. BLM contains DNA and metal ion binding regions, which coordinate with metal ions and generate free radicals, and it leads lipid

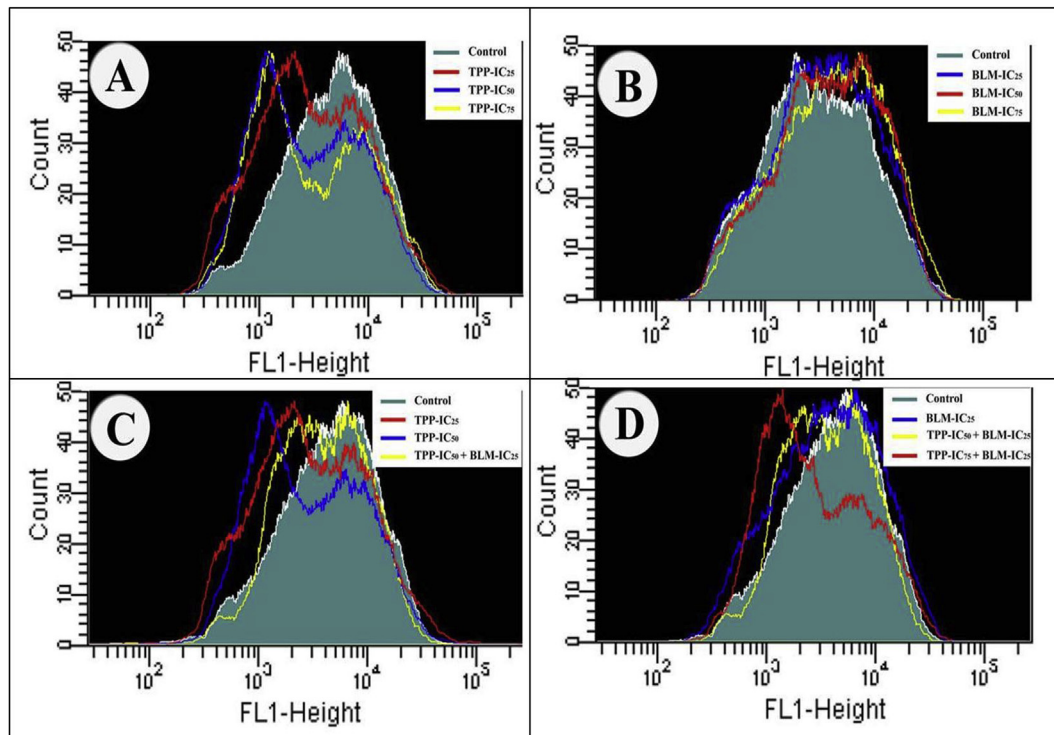


Fig. 5. Intracellular ROS measurement by flow cytometry using fluorescent the probe, 6-carboxy-2',7'-dichlorodihydrofluorescein diacetate, di(acetoxymethyl ester). A comparison of the intracellular ROS level changes, which are expressed as the mean fluorescent intensity in the cervical cells following TPP IC₅₀, BLM IC₅₀ or synergistic combination treatments (TPP in µg/mL + BLM in µM/ml) for 24 h is shown. The cells were trypsinized and the intracellular ROS was stained with a fluorescent probe (6-carboxy-2',7'-dichlorodihydrofluorescein diacetate, di(acetoxymethyl ester)). The intracellular ROS fluorescent intensity was measured from 10,000 events with flow cytometry. The experiments were repeated at least three times with similar results. Overlaid histograms representing the intracellular ROS levels from the TPP, BLM and TPP + BLM combination (TPP IC₂₅ in µg/mL + BLM IC₂₅ in µM/ml) treated as well as the untreated cells (control). (A) Control, TPP IC₂₅, TPP IC₅₀ and TPP IC₇₅; (B) Control, BLM IC₂₅, BLM IC₅₀ and BLM IC₇₅; (C) Control, TPP IC₂₅, TPP IC₅₀ and combination (TPP IC₅₀+BLM IC₂₅); (D) Control, BLM IC₂₅, (TPP IC₅₀+BLM IC₂₅) and (TPP IC₇₅+BLM IC₂₅).

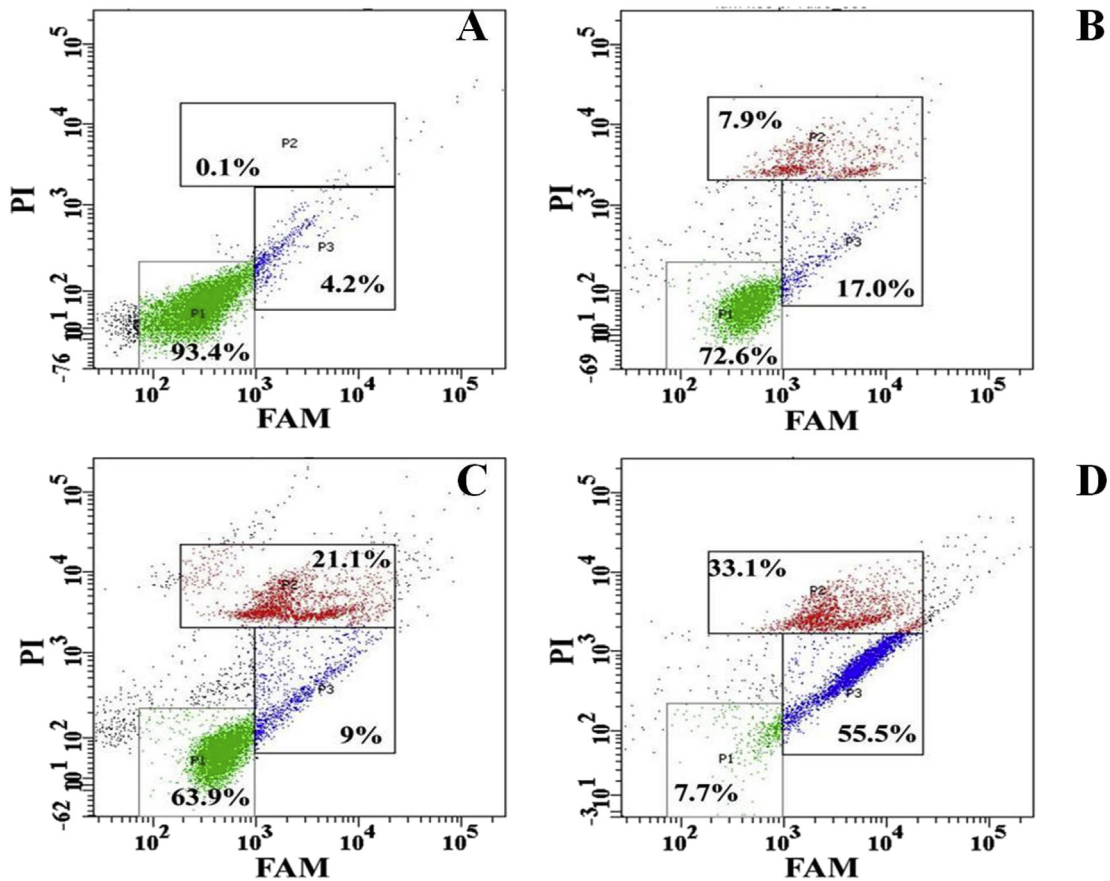


Fig. 6. Activated caspase detection by flow cytometry using fluorescently labeled inhibitors of caspases (FLICA) combined with plasma membrane permeability assay. Cervical cells were incubated with TPP IC₅₀, BLM IC₅₀ or a synergistic combination TPP + BLM dose TPP IC₅₀ + BLM IC₂₅ and TPP IC₇₅ + BLM IC₂₅ for 24 h. The treated SiHa cells were then processed according to the manufacturer's instruction (Polycaspase kit) at 37 °C in the dark. The fluorescence intensity was measured for 10,000 events with flow cytometry. Cervical cancer cells were untreated (A); TPP treated (B); BLE treated (C); or combination treated (TPP IC₂₅ + BLM IC₂₅) (D). Live cells (blue-colored populations) were negative for both FAM and PI. The early apoptotic cells (red-colored populations) were FAM-positive and PI-negative. The late apoptotic/secondary necrotic cells (green-colored populations) were positive for both FAM and PI. The experiments were repeated at least three times with similar results. (For interpretation of the references to colour in this figure legend, the reader is referred to the web version of this article).

peroxidation and other molecular oxidation. An excess of these generated free radicals trigger DNA cleavage, which leads to cancer cell death [13–15]. However, BLM can cause redox-mediated side effects in the normal cell, tissue and organs, including chemoresistance, senescence, and chronic toxicity, such as erythema, skin hyperpigmentation, striae, vesiculation, fever chills, hypotension, alopecia, stomatitis, fatigue, myocardial infarction, stroke, cardio-respiratory collapse and pulmonary toxicity [20,21,11,35,36]. Many recent reports indicated that RNA and protein metabolism are also distorted at high concentration of the BLM. It is possible that the combination of BLM and supplementary drugs, biologics, or non-dietary nutrition (like TPP) may exert synergistic action by targeting both key and reserve cellular mechanisms, simultaneously. Previous studies have demonstrated that a combination of chemotherapeutic drugs and phytochemicals could overcome the drugs' side effects and enhance their therapeutic activities [25,26,31]. TPP has attracted a great deal of interest because of its application for cancer prevention and as an adjuvant in cancer chemotherapy. Indeed, TPP can inhibit carcinogenesis by suppressing pro-oxidant enzyme expression, inhibiting target genes that are involved in cell proliferation, and inducing apoptosis [37,38]. Moreover, BLM is a well-known apoptotic inducer that triggers specific pathways that provide various hypothetical control chances and/or selected pathways to emphasize the synergistic cervical-tumor cell death. In the present study, the results

suggested that a combination of TPP and BLM might act synergistically and have therapeutic benefits. The synergistic activity of TPP-BLM may minimize the development of drug resistance and decrease toxicity while increasing efficacy. Our results suggest that TPP-BLM synergistically inhibited SiHa cell growth compared with individual TPP or BLM treatments. The CI and isobologram analysis for TPP-BLM revealed cytotoxic effects that were less additive. The difference between cytotoxicity and apoptosis is described by a sequence of characteristic morphological features, including cell shrinkage and fragmentation of the cell into membrane-bound apoptotic bodies and rapid phagocytosis by neighboring cells [39]. Our results suggested that the TPP-BLM treated SiHa cells displayed nuclear morphological changes, such as chromatin fragmentation, bi-/multinucleation, dot-like chromatin and apoptotic-bodies, which are characteristic of apoptotic cell death. Several genes are involved in and regulate apoptosis initiation, execution and regulation [40]. Apoptosis is triggered by p53 due to mitochondrial damage and high ROS levels. Moreover, the Bcl-2 protein family plays a crucial role in determining whether cells undergo apoptosis through caspases-9 and-3 [39–41].

Caspases are cysteine–aspartic acid specific proteases that are essential for programmed cell death. Caspase enzyme activation stimulates a sequence of reactions that are initiated in the cleavage of protein substrates and the consequent disassembly of the cell [42]. In the present study, caspase (including caspase-1, -3, -4, -5,

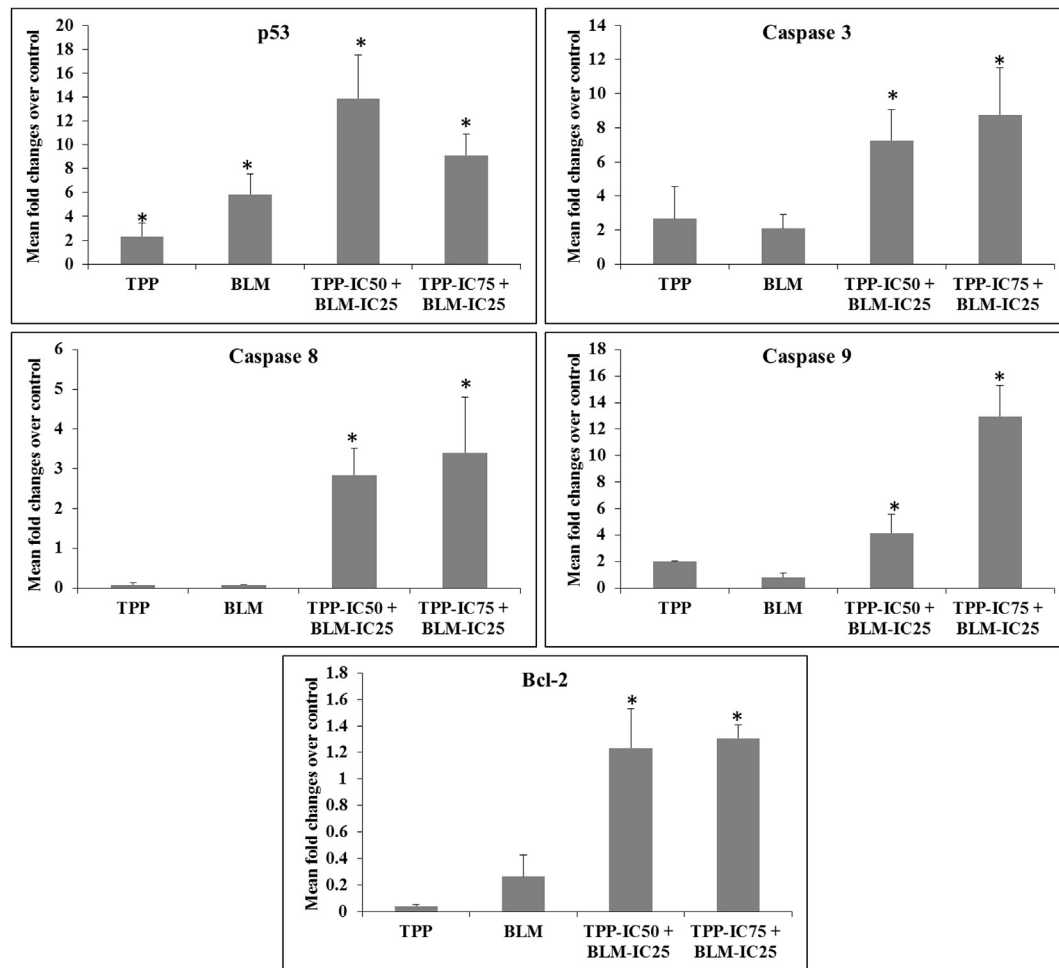


Fig. 7. Quantitative RT-PCR apoptotic marker genes analysis from the human cervical cancer cells. A comparison of the mRNA expression level changes, expressed as the mean fold change (as the ratio of the target gene to the reference gene [GAPDH]) in the cervical cells after 24 h of TPP IC₅₀, BLM IC₅₀ or synergistic combination exposure TPP IC₅₀ + BLM IC₂₅ and TPP IC₇₅ + BLM IC₂₅. The data represent the mean \pm SD of three determinations, each of which was performed in triplicate. The statistical analysis was performed using Student's t-tests ($p < 0.05$).

-6, -7, -8, and -9) activation was analyzed with fluorescently labeled inhibitors of caspases (FLICA), and plasma membrane permeability was evaluated with PI staining. The SiHa cells were treated with TPP-BLM (TPP IC₂₅ in $\mu\text{g}/\text{mL}$ + BLM IC₂₅ in $\mu\text{M}/\text{mL}$), which significantly increased the early (55.5% cells) and late apoptotic (33.1% cells) cells (Fig. 6) when compared with the control (untreated) and individual TPP (IC₅₀ dose 76.1 $\mu\text{g}/\text{mL}$) and BLM (IC₅₀ dose 9.44 $\mu\text{M}/\text{mL}$) treatments (Fig. 6A, B and C). Our results demonstrated that the TPP-BLM treatment induced the activation of all of the caspases at higher levels, which was associated with P53 upregulation. Previous studies revealed that the mechanism of action of BLM mainly involves the cleavage of mitochondrial DNA, which induces caspase-9 and -3 activation, which in turn leads to apoptosis [43,44]. Our results suggest that TPP-BLM synergistically activate caspase-9 in SiHa cells through ROS mediated-mitochondrial apoptosis. However, significant caspase-8 activation was found with the TPP, BLM and TPP-BLM treatments, which indicates that receptor-mediated apoptosis activation may have also been induced.

The network analysis for understanding the inter-connective and complex-multiple pathways were performed using bioinformatics approach. Recent system biological approaches explore the wide range of inter-connective gene regulatory networks and their specific mode of molecular mechanism for synergism. Our result of

network mapping and analysis suggest that more than 9 distinguished pathways were contributed through BLM and TPP exposure in human cancer cells. Particularly, as showed in the predicted protein and their relationships (Supporting data: Fig. S4.) such as death domain receptors, DNA damage & repair, extracellular apoptotic signals, pro-apoptotic genes, anti-apoptotic, positive & negative apoptotic regulatory genes, death domain receptors and caspases & regulators were involved. The results of functional enrichment analysis shows that more than 80 genes play a key role in the BLM induced and modulated by TPP (gallic acid, epigallocatechin, catechin, epicatechin, epigallocatechingallate and epicatechingallate) and were associated with modulation of redox signaling dependent pathways particularly. Indeed, TPP can inhibit and/or prevent carcinogenesis by modulating the expression of pro-oxidant enzymes, inhibiting target genes involved in cell proliferation, and inducing apoptosis through different mechanism of actions. The synergistic activity of BLM and TPP might have potency to minimize the development of drug resistance and decrease toxicity while increasing efficacy.

These findings suggest the existence of a threshold of cellular oxidation above which the apoptotic program is initiated. This threshold may vary depending on the dose level. However, the balance between the BLM-induced ROS and antioxidants (TPP) that are present in the cell at any given moment is likely crucial in

determining cell-fate decisions. Therefore, TPP-BLM might have potential therapeutic benefits as redox modifiers that are capable of directly inducing apoptosis specifically through ROS-mitochondrial junctions in cancer cells.

The anti-cancer properties of the BLM and TPP combination have rarely been investigated, until now. Our present study results provide strong evidence that the supplemental antioxidant, TPP, enhances the antitumor effects of BLM in uterine cervical cancer cells. Thus, clinical trials with uterine cervical cancer patients are needed to address the safety and efficacy of the antioxidant, TPP, and BLM combinational treatment with special reference to ROS mediated apoptosis.

In summary, our study demonstrated that TPP enhanced the therapeutic properties of BLM. Moreover, TPP-BLM synergistically inhibited uterine cervical cancer cell viability by decreasing proliferation through apoptosis. These results indicate that TPP may be an effective agent in combination with chemotherapy for treating uterine cervical cancer patients. Further investigations regarding the screening of several synergistic TPP and BLM combination doses that are useful as a cancer preventive or therapy are also needed.

Conflict of interest

The authors declare that there are no conflicts of interest.

Acknowledgments

We gratefully acknowledge the financial support of the Deanship of Scientific Research, King Saud University, Saudi Arabia (Grant No: RG-1435-044).

Appendix A. Supplementary data

Supplementary data related to this article can be found at <http://dx.doi.org/10.1016/j.cbi.2016.01.012>.

References

- [1] R. Siegel, J. Ma, Z. Zou, A. Jemal, *Cancer statistics 2014*, *CA Cancer J. Clin.* 64 (2014) 9–29.
- [2] J Ferlay, I Soerjomataram, M Ervik, et al. *GLOBOCAN 2012, Cancer Incidence and Mortality Worldwide: IARC CancerBase No. 11 2012*; <http://globocon.iarc.fr>. Accessed, 11/20, 2013.
- [3] H.S. Al-Eid, A.Z. Ali, *Cancer Incidence and Survival Report Saudi Arabia 2007, 2012*.
- [4] K. Munger, A. Baldwin, K.M. Edwards, H. Hayakawa, C.L. Nguyen, M. Owens, M. Grace, K.W. Huh, Mechanisms of human papillomavirus-induced oncogenesis, *J. Virol.* 78 (2004) 11451–11460.
- [5] R.S. Wong, Apoptosis in cancer: from pathogenesis to treatment, *J. Exp. Clin. Cancer Res.* 30 (2011) 87.
- [6] S. Elmore, Apoptosis: a review of programmed cell death, *Toxicol. Pathol.* 35 (2007) 495–516.
- [7] S. Fulda, K.M. Debatin, Extrinsic versus intrinsic apoptosis pathways in anti-cancer chemotherapy, *Oncogene* 25 (2006) 4798–4811.
- [8] J.C. Reed, Dysregulation of apoptosis in cancer, *J. Clin. Oncol.* 17 (1999) 2941–2953.
- [9] J. Fujimoto, Novel strategy of anti-angiogenic therapy for uterine cervical carcinomas, *Anticancer Res.* 29 (2009) 2665–2669.
- [10] W. Yaoxian, Y. Hui, Z. Yunyan, L. Yanqin, G. Xin, W. Xiaoke, Emodin induces apoptosis of human cervical cancer hela cells via intrinsic mitochondrial and extrinsic death receptor pathway, *Cancer Cell Int.* 13 (2013) 71.
- [11] S. Sleijfer, Bleomycin-induced pneumonitis, *Chest* 120 (2001) 617–624.
- [12] R.M. Burger, J. Peisach, S.B. Horwitz, Activated bleomycin. A transient complex of drug, iron, and oxygen that degrades DNA, *J. Biol. Chem.* 256 (1981) 11636–11644.
- [13] S.M. Hecht, Bleomycin: new perspectives on the mechanism of action, *J. Nat. Prod.* 63 (2000) 158–168.
- [14] S. Neidle, Molecular Aspects of Anticancer Drug DNA Interactions. 2, CRC Press, 1994.
- [15] B. Roy, C. Tang, M.P. Alam, S.M. Hecht, DNA methylation reduces binding and cleavage by bleomycin, *Biochemistry* 53 (2014) 6103–6112.
- [16] A. Cort, M. Timur, E. Ozdemir, E. Kucuksayan, T. Ozben, Synergistic anticancer activity of curcumin and bleomycin: an in vitro study using human malignant testicular germ cells, *Mol. Med. Rep.* 5 (2012), 1481–1486.
- [17] E.L. Delphinegimonet, H. Bobichon, Induction of apoptosis by bleomycin in p53-null HL-60 leukemia cells, *Int. J. Oncol.* 24 (2004) 313–319.
- [18] S. Brahim, K. Abid, A. Kenani, Role of carbohydrate moiety of bleomycin-A2 in caspase-3 activation and internucleosomal chromatin fragmentation in apoptosis of laryngeal carcinoma cells, *Cell Biol. Int.* 32 (2008) 171–177.
- [19] J. Chen, J. Stubbe, Bleomycins: towards better therapeutics, *Nat. Rev. Cancer* 5 (2005) 102–112.
- [20] J. Hay, S. Shahzeidi, G. Laurent, Mechanisms of bleomycin-induced lung damage, *Arch. Toxicol.* 65 (1991) 81–94.
- [21] I. Vorechovsky, M. Munzarova, J. Lokaj, Increased bleomycin-induced chromosome damage in lymphocytes of patients with common variable immunodeficiency indicates an involvement of chromosomal instability in their cancer predisposition, *Cancer Immunol. Immunother.* 29 (1989) 303–306.
- [22] N. Khan, H. Mukhtar, Multitargeted therapy of cancer by green tea polyphenols, *Cancer Lett.* 269 (2008) 269–280.
- [23] M. Athar, J.H. Back, X. Tang, K.H. Kim, L. Kopelovich, D.R. Bickers, A.L. Kim, Resveratrol: a review of preclinical studies for human cancer prevention, *Toxicol. Appl. Pharmacol.* 224 (2007) 274–283.
- [24] H. Kaiserova, T. Simunek, W.J. van der Vijgh, A. Bast, E. Kvasnickova, Flavonoids as protectors against doxorubicin cardiotoxicity: role of iron chelation, antioxidant activity and inhibition of carbonyl reductase, *BBA-Mol. Basis Dis.* 1772 (2007) 1065–1074.
- [25] G. Scambia, F.O. Ranelletti, P. Benedetti-Panici, R. De Vincenzo, G. Bonanno, et al., Quercetin potentiates the effect of adriamycin in a multidrug-resistant MCF-7 human breast-cancer cell line: P-glycoprotein as a possible target, *Cancer Chemother. Pharmacol.* 34 (1994) 459–464.
- [26] R. Hoffman, L. Graham, E.S. Newlands, Enhanced anti-proliferative action of busulphan by quercetin on human leukaemia cell line K562, *Br. J. Cancer* 59 (1989) 347–348.
- [27] S.J. Hosseini-mehr, M. Rostamnezad, R.V. Ghafari, Epicatechin enhances anti-proliferative effect of bleomycin in ovarian cancer cell, *Res. Mol. Med.* 1 (2013) 24–27.
- [28] B. Frei, J.V. Higdon, Antioxidant activity of tea polyphenols in vivo: evidence from animal studies, *J. Nutr.* 133 (2003) 3275S–3284S.
- [29] N. Khan, H. Mukhtar, Multitargeted therapy of cancer by green tea polyphenols, *Cancer Lett.* 269 (2008) 269–280.
- [30] N. Khan, H. Mukhtar, Tea polyphenols for health promotion, *Life Sci.* 81 (2007) 519–533.
- [31] V.S. Periasamy, A.A. Alshatwi, Tea polyphenols modulate antioxidant redox system on cisplatin-induced reactive oxygen species generation in a human breast cancer cell, *Basic Clin. Pharmacol. Toxicol.* 112 (2013) 374–384.
- [32] X. Chen, Y. Li, Q. Lin, Y. Wang, H. Sun, J. Wang, X. Dong, Tea polyphenols induced apoptosis of breast cancer cells by suppressing the expression of Survivin, *Sci. Rep.* 4 (2014) 4416.
- [33] N. Sriram, S. Kalayarasan, G. Sudhandiran, Epigallocatechin-3-gallate exhibits anti-fibrotic effect by attenuating bleomycin-induced glycoconjugates, lysosomal hydrolases and ultrastructural changes in rat model pulmonary fibrosis, *Chem. Biol. Interact.* 180 (2009) 271–280.
- [34] T.C. Chou, P. Talalay, Quantitative analysis of dose–effect relationships: the combined effects of multiple drugs or enzyme inhibitors, *Adv. Enzyme Regul.* 22 (1984) 27–55.
- [35] E. Chu, V.T. DeVita Jr., *Cancer Chemotherapy Drug Manual*, Jones and Bartlett, Boston, Mass, USA, 2011.
- [36] A.A. Ferrando, A.M. Pendas, E. Llano, G. Velasco, R. Lidereau, C. Lopez-Otın, Gene characterization, promoter analysis, and chromosomal localization of human bleomycin hydrolase, *J. Biol. Chem.* 272 (1997) 33298–33304.
- [37] L. Ann Beltz, D. Kay Bayer, A. Lynn Moss, I. Mitchell Simet, Mechanisms of cancer prevention by green and black tea polyphenols, *Anti-Cancer Agents Med. Chem.* 6 (2006) 389–406.
- [38] S.B. Moyers, N.B. Kumar, Green tea polyphenols and cancer chemoprevention: multiple mechanisms and endpoints for phase II trials, *Nutr. Rev.* 62 (2004) 204–211.
- [39] J.F.R. Kerr, A.H. Wyllie, A.R. Currie, Apoptosis: a basic biological phenomenon with wide-ranging implications in tissue kinetics, *Br. J. Cancer* 26 (1972) 239–257.
- [40] S.J. Riedl, Y. Shi, Molecular mechanisms of caspase regulation during apoptosis, *Nat. Rev. Mol. Cell Biol.* 5 (2004) 897–907.
- [41] M.S. Shabnam, R. Srinivasan, A. Wali, S. Majumdar, K. Joshi, D. Behera, Expression of p53 protein and the apoptotic regulatory molecules Bcl-2, Bcl-X_L, and Bax in locally advanced squamous cell carcinoma of the lung, *Lung Cancer* 45 (2004) 181–188.
- [42] J. Wang, M.J. Lenardo, Roles of caspases in apoptosis, development, and cytokine maturation revealed by homozygous gene deficiencies, *J. Cell Sci.* 113 (2000) 753–757.
- [43] S.S. Brar, J.N. Meyer, C.D. Bortner, B. Van Houten, W.J. Martin II, Mitochondrial DNA-depleted A549 cells are resistant to bleomycin, *Am. J. Physiol. Lung Cell. Mol. Physiol.* 303 (2012) L413–L424.
- [44] F. Morel, M. Renoux, P. Lachaume, S. Alziari, Bleomycin-induced double-strand breaks in mitochondrial DNA of *Drosophila* cells are repaired, *Mut. Res.* 637 (2008) 111–117.